SPANDIDOS PUBLICATIONS

ONCOLOGY LETTERS 11: 2773-2779, 2016

ASF-4-1 fibroblast-rich culture increases chemoresistance and mTOR expression of pancreatic cancer BxPC-3 cells at the invasive front *in vitro*, and promotes tumor growth and invasion *in vivo*

MASAYA FUJIWARA*, KAZUKI KANAYAMA*, YOSHIFUMI S. HIROKAWA and TAIZO SHIRAISHI

Department of Oncological Pathology, Institute of Molecular and Experimental Medicine, Mie University Graduate School of Medicine, Tsu, Mie 514-8507, Japan

Received January 28, 2015; Accepted November 17, 2015

DOI: 10.3892/ol.2016.4289

Abstract. Pancreatic cancer develops dense stromal tissue through the desmoplastic reaction. The aim of the present study was to assess the effects of a fibroblast-rich environment on the malignant potential of pancreatic cancer. Cells from the human pancreatic cancer cell line BxPC-3 were mixed at a ratio of 1:3 (fibroblast-rich) or 1:1 (fibroblast-poor) with cells from the human skin fibroblast line ASF-4-1. In the fibroblast-rich co-culture, tumor budding was observed and BxPC-3 cells were found to be more resistant to gemcitabine than those in the fibroblast-poor co-culture. Immunohistochemistry revealed that the expression of mammalian target of rapamycin was increased at the invasive front of fibroblast-rich co-cultures. In addition, in mouse xenografts of fibroblast-rich co-cultures, tumors were larger and had a higher Ki-67 index compared with that of the fibroblast-poor co-culture xenografts. These results indicate that fibroblast-rich co-cultures may promote the malignant potential of the pancreatic cancer cell line BxPC-3, both *in vitro* and *in vivo*.

Introduction

Pancreatic cancer is the fourth most common cause of cancer-associated mortality worldwide (1). The disease is highly aggressive as it is often discovered late and typically develops resistance to conventional therapy (2). The five-year survival rate is <5%, indicating a poor prognosis for all stages (1,3).

In colorectal cancer and early breast cancer, it has been found that the proportion of stromal cells within the primary tumor has prognostic value (4,5). Pancreatic cancer tissue is characterized by its enrichment of stromal cells. Furthermore, pancreatic stellate cells, which are myofibroblast-like cells found in the areas of the pancreas that have exocrine function, are critical in the desmoplastic reaction, resulting in cancer cell progression (6). However, it has not been investigated whether the pancreatic cancer cell-to-stromal cell ratio in the primary tumor is a prognostic factor.

In cancer biology, the nature of the cancer microenvironment is important (7). The cancer microenvironment, which is formed by tumor cells and tumor-mediated interactions with stromal cells and the extracellular matrix (7), supports malignant growth and invasion (6). Stromal fibroblasts promote pancreatic cancer cell proliferation (8). In squamous cell carcinoma, fibroblasts lead collective cancer cell invasion into three-dimensional (3D) culture (9). For the analysis of cellular function and interaction, 3D culture systems have been developed to mimic the *in vivo* architecture of the cancer microenvironment in natural organs and tissues (10).

Tumor budding is defined as the presence of individual or small clusters (1-5 cells) of de-differentiated cancer cells around the invasive front (11,12). Budding is an independent prognostic factor in pancreatic cancer, as well as colorectal and esophageal cancers (11,13,14). Tumor budding is closely correlated with nodal metastasis (15), and is thought to reflect the process of epithelial-mesenchymal transition (EMT), which increases the capacity for migration and invasion (16,17).

Mammalian target of rapamycin (mTOR) controls the size of cells through its modulation of the rate at which ribosomal proteins are synthesized (18). mTOR expression is associated with cancer progression and chemoresistance (19). Therefore, investigating the expression of mTOR in pancreatic cancer is important in order to better understand the biology of the disease.

In the present study, a 3D co-culture that mimicked the microenvironment of pancreatic cancer was established. The co-culture consisted of human pancreatic cancer cells

Correspondence to: Dr Yoshifumi S. Hirokawa, Department of Oncological Pathology, Institute of Molecular and Experimental Medicine, Mie University Graduate School of Medicine, 2-174 Edobashi, Tsu, Mie 514-8507, Japan
E-mail: ultray2k@clin.medic.mie-u.ac.jp

*Contributed equally

Key words: pancreatic cancer, fibroblast, mTOR, budding, three-dimensional co-culture

(BxPC-3 cell line) and skin fibroblasts (ASF-4-1 cell line) with extracellular matrix collagen gel and Matrigel. The effect of a fibroblast-rich environment on the malignant potential of pancreatic cancer was investigated by analyzing tumor budding and mTOR expression through immunohistochemical staining of the culture.

Materials and methods

Cells and cell culture. The human pancreatic cancer cell line BxPC-3 was obtained from the RIKEN Bioresource Center Cell Bank (Tsukuba, Japan), and human skin fibroblast ASF-4-1 cells were obtained from the Japanese Collection of Research Bioresources Cell Bank (National Institutes of Biomedical Innovation, Health and Nutrition; Osaka, Japan).

Cells were cultured in RPMI-1640 medium (Sigma-Aldrich, St. Louis, MO, USA) supplemented with 10% fetal bovine serum (FBS; Invitrogen, Thermo Fisher Scientific, Carlsbad, CA, USA) and antibiotics (100 U/ml penicillin and 100 μg/ml streptomycin; Nacalai Tesque, Inc., Kyoto, Japan) in a humidified atmosphere of 5% CO_2 at 37˚C.

3D Matrigel and collagen invasion assay. Matrigel (#354234; BD Biosciences, Franklin Lakes, NJ, USA) was diluted at a 1:3 ratio with AteloCell (#KOU-RPM-02; Koken Co., Ltd., Tokyo, Japan) and mixed. The mixture was then placed in Falcon Cell Culture Inserts (8 μl pore size; #353097; Corning, Inc., Corning, NY, USA) in 24-well plates (100 μl/well). Following incubation for 1 h at 37˚C, 500 μl of supplemented RMPI-1640 medium (described above) was added to the bottom of each well. BxPC-3 cells were adjusted to a final concentration of $1.0x10^6$ cells/ml with FBS-free medium, and suspended gently on the 3D Matrigel (as described above) for the collagen invasion assay. Each well contained $1.0x10^5$ pancreatic cancer cells. For the addition of ASF-4-1 cells, the number of these fibroblasts was adjusted to a 1:1 (fibroblast-poor) or 3:1 (fibroblast-rich) ratio with BxPC-3 cells in 100 μl of medium. Gemcitabine (10 μM) was added 24 h after seeding, by which point all cells had aggregated.

Following a 48-h incubation, the cells were assessed under light microscopy (BX50F; Olympus Corporation, Tokyo, Japan). The polycarbonate membranes at the bottom of each chamber were cut and fixed in 10% formalin for 6 h, and subsequently fixed with HOLD GEL 110 (Ebis1 kit; Asiakizai Co., Ltd., Tokyo, Japan) and embedded in paraffin. Blocks were sliced into 3 μm-thick sections, stained with hematoxylin and eosin and subjected to immunohistochemistry. Invasion assays were performed a minimum of three times.

Immunohistochemistry and reagents. Automated immunohistochemical staining was performed with a BenchMark LT slide stainer (Ventana Medical Systems, Inc., Tucson, AZ, USA). After pretreatment with citrate buffer (Ventana Medical Systems, Inc.) for 60 min, sections were incubated for 32 min at 37˚C with the following primary antibodies: Mouse monoclonal antibodies against cytokeratin 18 (CK18; #sc-6259; Santa Cruz Biotechnology, Inc., Dallas, TX, USA; dilution, 1:100), E-cadherin (#18-0223; Invitrogen, Thermo Fisher Scientific; dilution, 1:50), caspase-cleaved CK18 (M30 CytoDEATH; #10700; PEVIVA, Stockholm, Sweden; dilution, 1:100), vimentin (#M0725; Dako, Glostrup, Denmark; dilution, 1:100), Ki-67 (MIB-1; #08-1156; Invitrogen, Thermo Fisher Scientific; ready-to-use); rabbit polyclonal anti-CD31 (#ab28364; Abcam, Cambridge, MA, USA; dilution, 1:40) and rabbit monoclonal anti-mTOR (#2983; Cell Signaling Technology, Inc., Danvers, MA, USA; dilution, 1:100). The mTOR inhibitor rapamycin was obtained from Abcam (#ab120224). Gemcitabine was purchased from Wako (#077-05671; Wako Pure Chemical Industries, Ltd., Osaka, Japan). Ki-67 proliferation indices were measured by nuclear staining with the MIB-1 monoclonal antibody. For chromogenic detection iVIEW DAB Detection kit (#760-091; Ventana Medical Systems, Inc.) was used. This kit included secondary antibodies, which were a mixture of biotin-conjugated goat anti-mouse immunoglobulin (Ig)G polyclonal antibody, anti-mouse IgM polyclonal antibody and anti-rabbit IgG polyclonal antibody. Samples were incubated with secondary antibody at 37˚C for 8 min. The chromogenic reaction was performed using 3,3'-diaminobenzidine and horseradish peroxidase-conjugated streptavidin (both taken from the iVIEW DAB Detection kit). Evaluation of mTOR expression at the invasive front was scored by the percentage and intensity of staining. Staining percentage was scored as follows: 0 points, <1%; 1 point, 1-20%; 2 points, 21-50%; and 3 points, >50%. Staining intensity was scored as follows: 3 points, strong; 2 points, intermediate; 1 point, weak; and 0 points, negative. The sum of these two scores served as the total score.

Xenograft and tissue preparation. Male severe combined immunodeficiency (SCID) mice (n=20; weight, 23-25 g) were housed (5 mice per cage) in pathogen-free conditions and exposed to 12 h light/dark cycles, with *ad libitum* access to food and water. At 8 weeks of age the mice were used. For implantation, an incision was made in the backs of the mice, and $1.0x10^5$ BxPC-3 cells with ASF-4-1 cells (1:1 or 1:3 ratio) from the 48-h 3D co-cultures were transplanted into the subcutaneous tissue of the mice. Every week, tumor sizes were recorded. After 4, 6, 8 or 10 weeks, five mice were sacrificed by CO_2 inhalation, the tumors were harvested, embedded in paraffin and cut into 3-μm sections. The sections were then stained with hematoxylin and eosin for immunohistochemical analysis.

All animal experiments were performed in accordance with the guidelines approved by the ethics committees of Mie University (Tsu, Japan).

Statistical analysis. Mean tumor size and area were compared between groups, and a two-tailed independent sample Student's *t*-test was applied. $P<0.01$ was considered to indicate a statistically significant difference.

Results

Fibroblast-rich co-cultures exhibit tumor budding and greater resistance of BxPC-3 cells to gemcitabine than cells in fibroblast-poor co-cultures. To analyze the association between pancreatic cancer cells and fibroblasts, a 3D co-culture system closely mimicking the physiological interactions in tissue was established. BxPC-3 cells co-cultured with an equal number of ASF-4-1 cells were able to migrate into the gel,

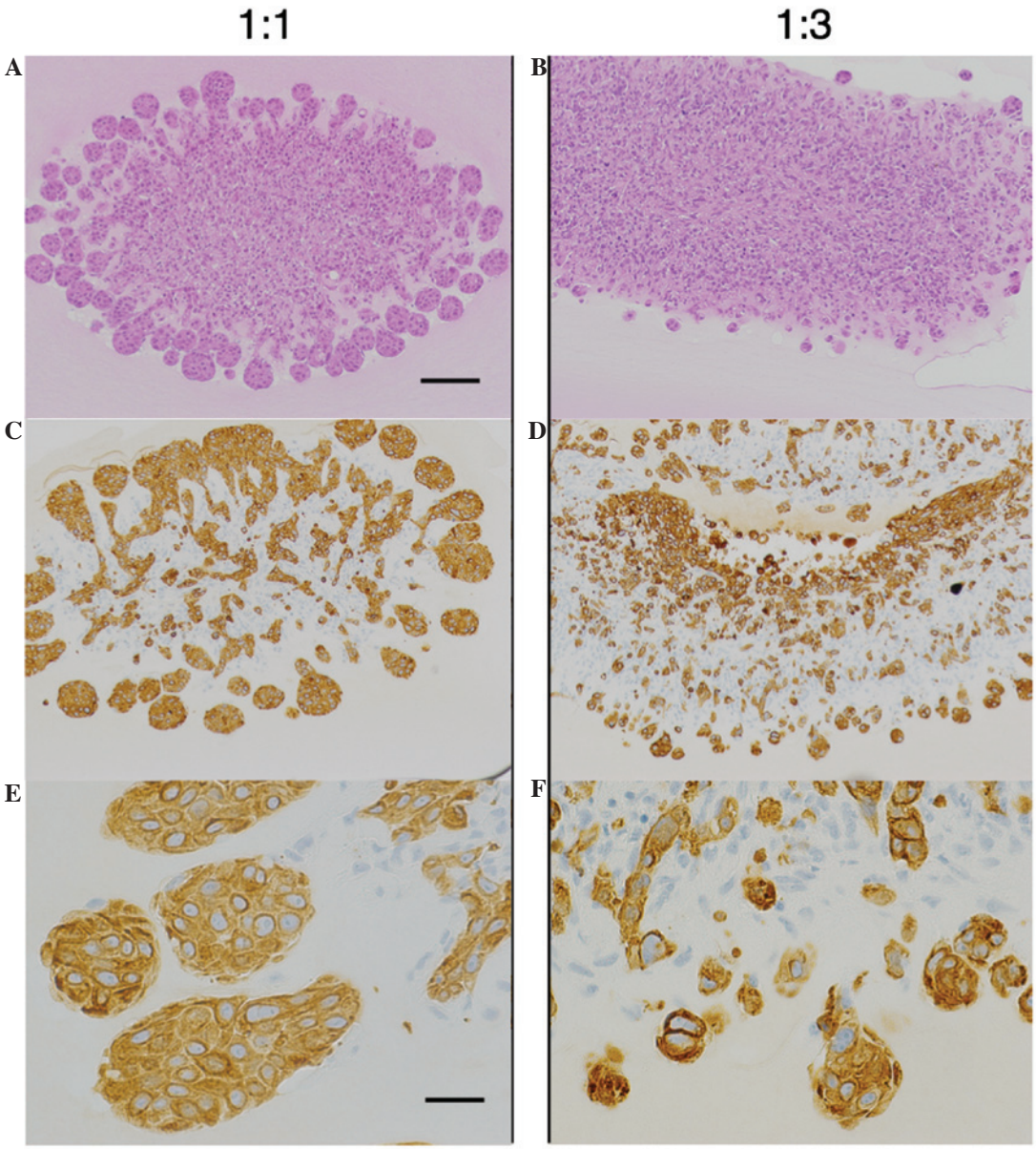

Figure 1. A comparison of co-cultured models with various ratio of ASF-4-1 cells. (A and B) Hematoxylin and eosin staining and (C-F) immunohistochemical staining for CK18. (A, C and E) BxPC-3 cells co-cultured with an equivalent number of ASF-4-1 cells (1:1 co-culture) formed characteristic structures; BxPC-3 cells were CK18-positive and demonstrated an invasive front. (B, D and F) BxPC-3 cells were mixed at a ratio of 1:3 with ASF-4-1 cells; BxPC-3 cells formed small clusters (tumor budding) around the invasive front. (A-D) scale bar, 100 μm; (E and F) scale bar, 25 μm. CK18, cytokeratin 18.

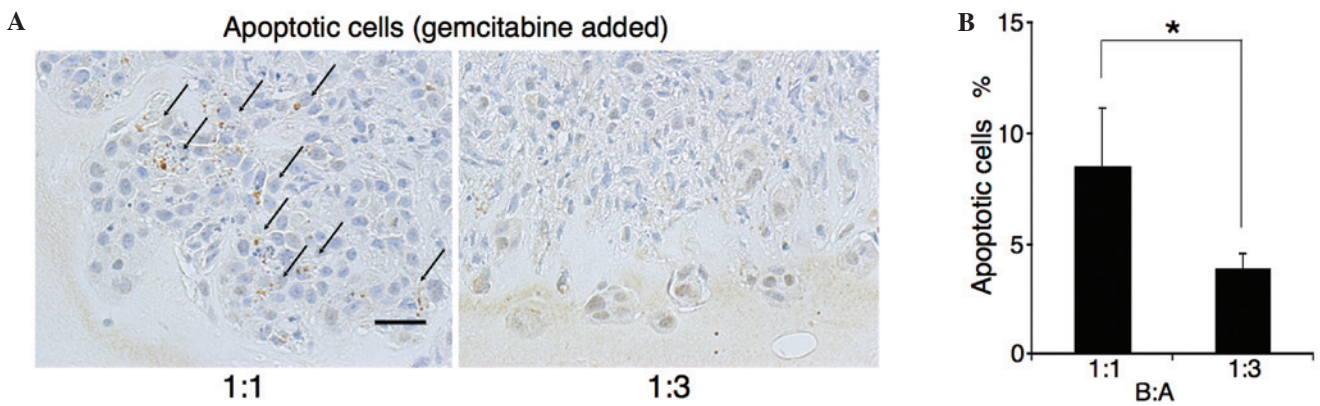

Figure 2. Estimation of chemoresistance by measuring apoptotic cells positive for staining by M30 CytoDEATH. (A) Immunohistochemical assessment for M30 CytoDEATH in three-dimensional culture with gemcitabine (10 μM) (scale bar, 50 μm). Gemcitabine was added 24 h after seeding when all cells had aggregated. Arrows indicate apoptotic cells. (B) M30 CytoDEATH-positive BxPC-3 cells in B:A=1:3 co-cultures were fewer than in B:A=1:1 co-cultures (*P<0.01). B:A, BxPC-3:ASF-4-1.

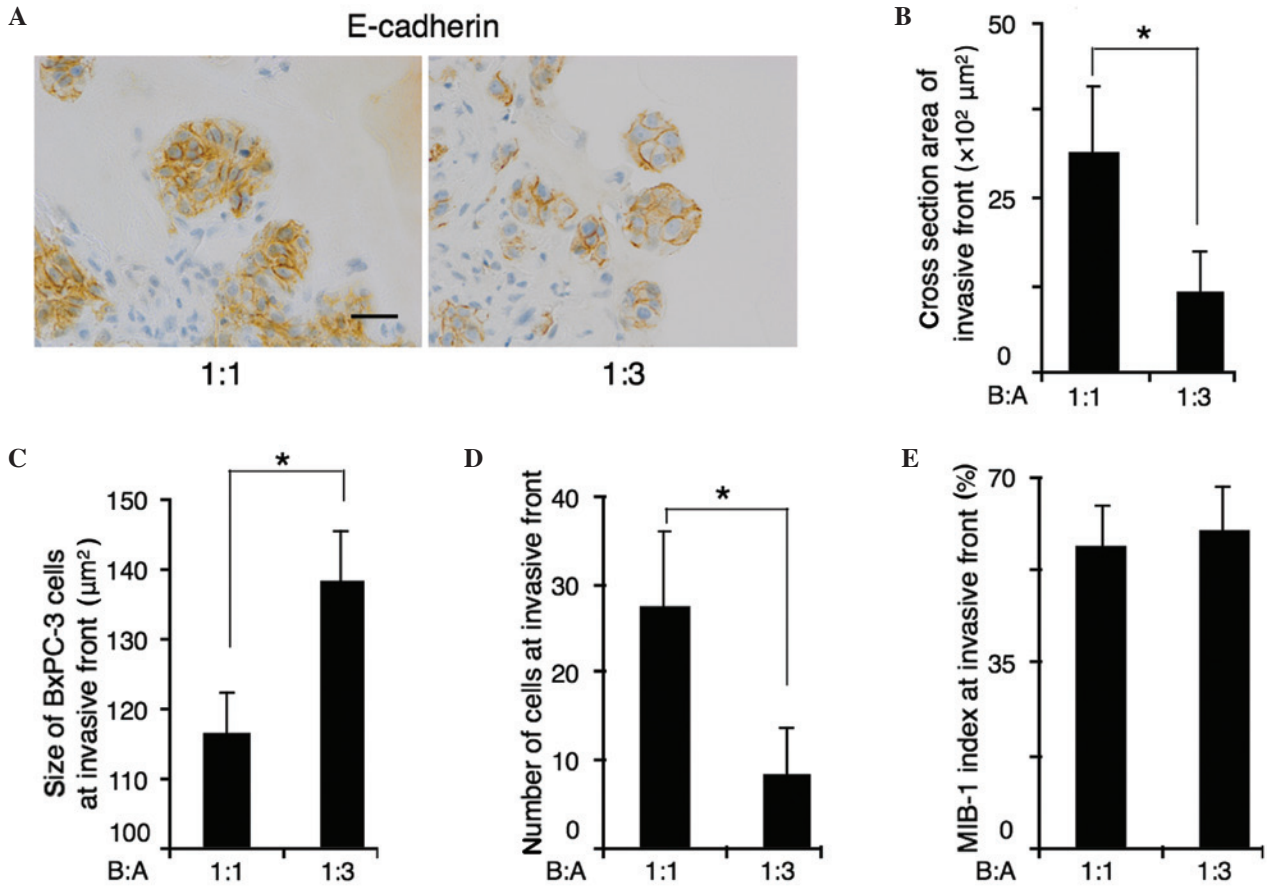

Figure 3. A comparison of BxPC-3 cell size at the invasive front with varying ratios of ASF-4-1 cells. (A) Immunohistochemical staining for E-cadherin (scale bar, 25 μm); BxPC-3 cell size was measured (image analysis cross section area divided by the number of BxPC-3 cells at the invasive front) along with E cadherin positive membranes. At the invasive front, (B) the cross-sectional area and (C) cell number in fibroblast-rich co-culture were reduced compared with those in fibroblast-poor co-culture. (D) The size of cells at the invasive front in fibroblast-rich co-culture were larger than that in fibroblast-poor co-culture. (E) No difference in MIB-1 indices was observed between the two co-cultures. *P<0.01. B:A, BxPC-3:ASF-4-1.

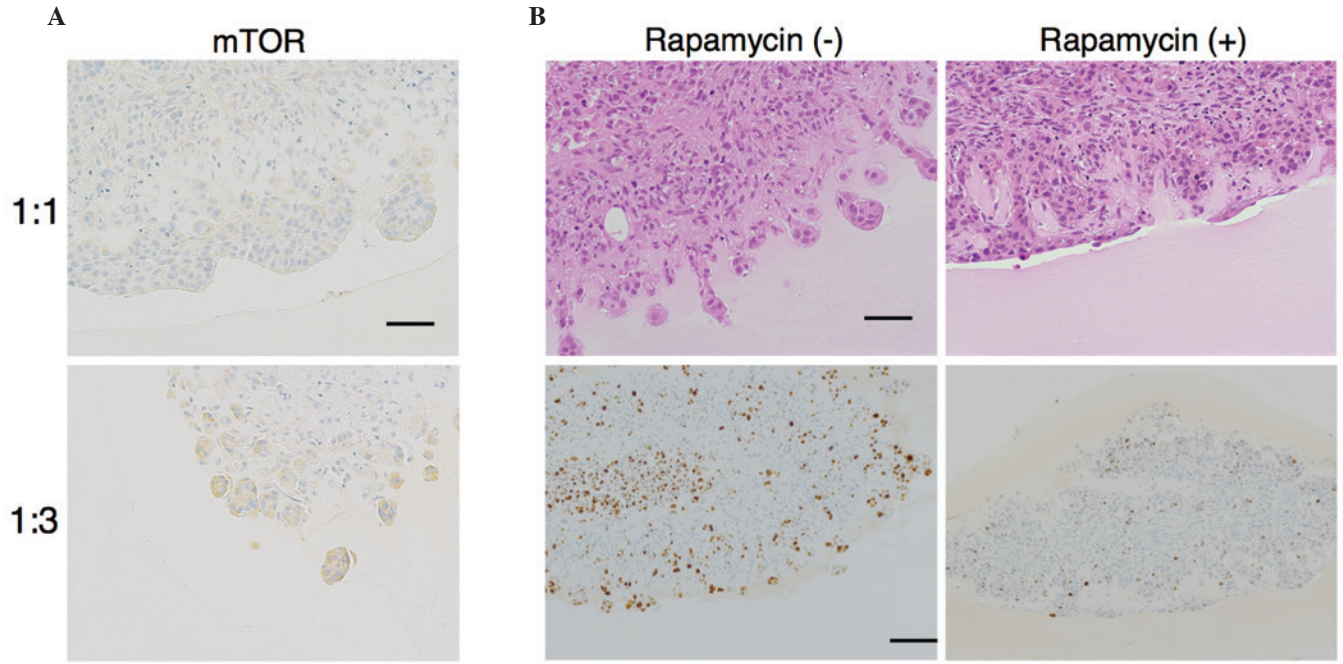

Figure 4. mTOR expression at the invasive front and the effect of inhibition of mTOR by rapamycin. (A) Immunohistochemical staining for mTOR (scale bar, 50 μm) revealed that mTOR total score (as described in the materials and methods) was increased at the invasive front from B:A=1:1 to B:A=1:3 co-cultures (P<0.001). (B) Hematoxylin and eosin staining (top row; scale bar, 50 μm) and immunohistochemical assessment of MIB-1 (bottom row; scale bar, 100 μm). Rapamycin, an inhibitor of mTOR, was added following the aggregation of BxPC-3 cells and ASF-4-1 cells on the gel. Rapamycin prevented invasive front formation and proliferation in B:A=1:3 cultures. mTOR, mammalian target of rapamycin; B:A, BxPC-3:ASF-4-1.

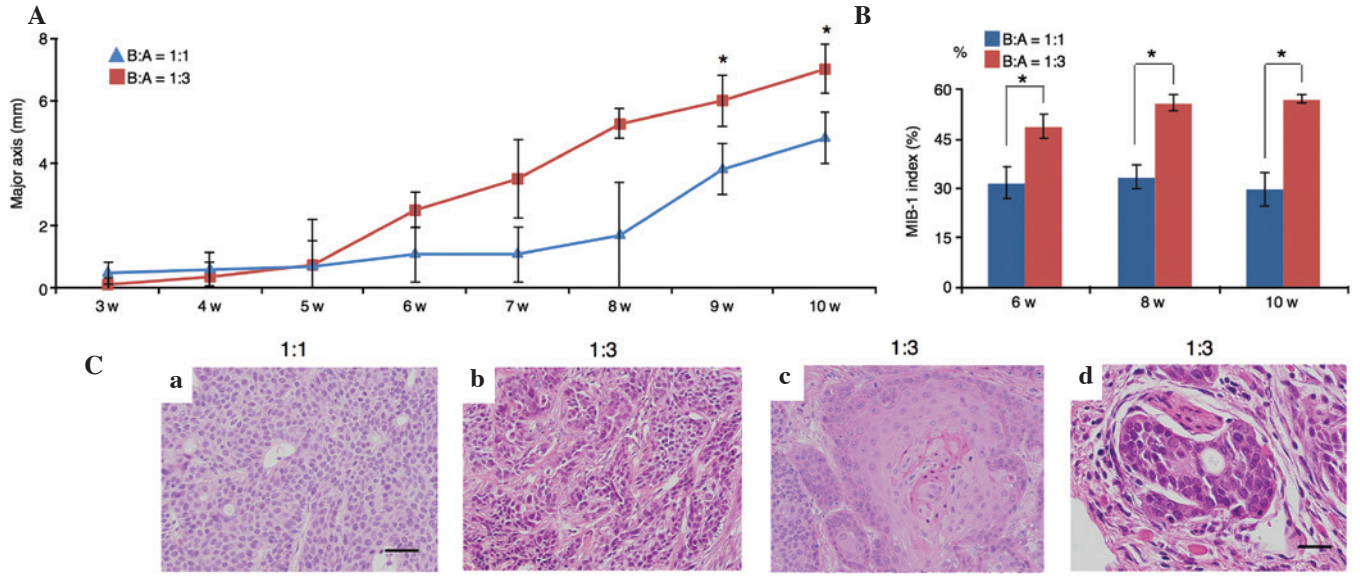

Figure 5. Comparison of tumor growth speed, and estimation of the MIB-1 indices and histological features. (A) Tumor growth was assessed using the major axis of tumor diameter (mm). In a xenograft model in severe combined immunodeficiency mice, tumor growth of fibroblast-rich co-cultures was faster than that achieved by fibroblast-poor co-cultures, particularly at 9 and 10 weeks (*P<0.01). (B) The MIB-1 indices at 6, 8 and 10 weeks using B:A=1:3 co-cultures were significantly higher than those of the B:A=1:1 co-cultures (*P<0.01). (C) Histological features of tumors from xenografted mice [hematoxylin and eosin staining; B:A cell ratio indicated above images; (a-c) scale bar, 50 μm; (d) scale bar, 25 μm]: (a) BxPC-3 cells from fibroblast-poor co-cultures had small round nuclei; (b) in fibroblast-rich co-cultures, tumor cells exhibited pleomorphism; (c) BxPC-3 cells with rich fibroblasts exhibited differentiation to squamous cell carcinoma; (d) neural invasion was observed only in tumors initiated by fibroblast-rich co-cultures. B:A, BxPC-3:ASF-4-1. w, weeks.

and formed a characteristic invasive front at the advancing edge of the tumor (Fig. 1A-C). The invasive front was defined as the most external cancer cell nest. To study whether fibroblasts promoted the malignant potential of BxPC-3 cells ('B'), increased numbers of ASF-4-1 cells ('A') were co-cultured with a constant number of BxPC-3 cells. In B:A co-cultures with a 1:3 ratio, tumor budding was observed around the invasive front (Fig. 1D-F). Budding was defined as small clusters of de-differentiated cancer cells around the invasive front of the lesion; this correlates with poor prognosis in pancreatic cancer as well as colorectal and esophageal cancers (12-14). The number of buds was higher in B:A=1:3 co-cultures than in B:A=1:1 co-cultures, as demonstrated by CK18-positive findings, which indicate the distribution of cancer cells (Fig. 1E and F).

Gemcitabine (10 μM) was added 24 h after seeding, by which point all cells had aggregated. Following a further 24 h, apoptotic/CK18-positive cells were counted. As observed in the first part of the experiment, almost all cells at the invasive front were cancer cells (Fig. 1C and F). The M30 CytoDEATH antibody recognizes human caspase-cleaved CK18, which is not observed in viable cells (20). The percentage of M30 CytoDEATH-positive cells at the invasive front was assessed (Fig. 2A). In B:A=1:1 co-cultures, the percentage of M30 CytoDEATH-positive cells was 8.5%, whilst that in B:A=1:3 co-cultures was 3.9% (P=0.003) (Fig. 2B). Thus, BxPC-3 cells in B:A=1:3 co-cultures were more resistant to gemcitabine than cells in B:A=1:1 co-cultures.

BxPC-3 cells at the invasive front of fibroblast-rich co-cultures are larger than that in fibroblast-poor cultures. Immunohistochemical staining for E-cadherin was used to allow measurement of the cross sectional area of the invasive front. The cross sectional area was calculated using the image analyzing software, DP2-BSW (Olympus Corporation), by tracing the outline of invasive front. The size of BxPc-3 cells was calculated by dividing the cross sectional area of the invasive front by the number of BxPc-3 cells at the invasive front (Fig. 3A). The cross-sectional area of the invasive front was decreased in B:A=1:3 co-cultures compared with B:A=1:1 co-cultures. The average area of the cross-section of the invasive front was 3,156 μm^2 in B:A=1:1 co-cultures, and 1,155 μm^2 in B:A=1:3 co-cultures (P<0.001) (Fig. 3B). Furthermore, the number of the cells at the invasive front was decreased in B:A=1:3 co-cultures. In B:A=1:1 co-cultures, the average number of BxPC-3 cells at the invasive front was 23, whereas in B:A=1:3 co-cultures showed an average of 8 cells (P<0.001) (Fig. 3C). Reducing the number of cells in the invasive front was responsible for decreasing the size of the invasive front in B:A=1:3 co-cultures. However, the average size of each BxPC-3 cell at the invasive front of B:A=1:3 co-cultures was 138±5.8 μm^2, which were larger than that of B:A=1:1 co-cultures (116±5.8 μm^2), despite the reduced cross-sectional area of the invasive front (Fig. 3D). MIB-1 indices remained unaltered, regardless of the number of fibroblasts (Fig. 3E).

mTOR is increased at the invasive front in fibroblast-rich co-cultures, and mTOR inhibition suppresses invasive front formation and proliferation. As mTOR controls the size of cells through regulating the rate of protein synthesis of ribosomes, we hypothesized that the increased size of cells at the invasive front in B:A=1:3 co-cultures was related to mTOR. Immunohistochemical staining revealed that expression of mTOR was increased at the invasive front in B:A=1:3 co-cultures (total

score = 5.666±0.516) relative to that in B:A=1:1 co-cultures (total score = 0.666±1.032) (Fig. 4A).

Treatment with rapamycin (100 nM), an mTOR inhibitor, was observed to prevent invasive front formation in B:A=1:3 co-cultures (Fig. 4B). The MIB-1 index at the edge of the front without rapamycin in fibroblast-rich co-cultures was 50%, whereas the MIB-1 index with rapamycin was 7% (Fig. 4B). Thus, the proliferation rate differed significantly in the presence or absence of rapamycin (P<0.001). These results indicate that mTOR expression in BxPC-3 cells may modulate the malignant potential of the cancer cells.

A fibroblast-rich environment promotes tumor growth and invasion in xenograft models. In xenograft models using SCID mice, tumor growth initiated by B:A=1:3 co-cultures was more rapid than that initiated by B:A=1:1 co-cultures (P=0.005; Fig. 5A). Additionally, the MIB-1 indices at 6, 8 and 10 weeks in B:A=1:3 co-cultures were significantly higher than those in B:A=1:1 co-cultures (P=0.005; Fig. 5B).

Upon examination of the transplanted B:A=1:1 co-cultures, it was observed that BxPC-3 cells exhibited homogeneous proliferation and had small, round nuclei; these cells did not infiltrate into peripheral tissues (Fig. 5Ca). However, following transplantation of B:A=1:3 co-cultures, BxPC-3 cells exhibited marked nuclear atypia and pleomorphism (Fig. 5Cb). Furthermore, differentiation to squamous cell carcinoma (Fig. 5Cc) and neural invasion (Fig. 5Cd) were observed in the B:A=1:3 co-culture group.

There was no significant difference in BxPC-3 mTOR expression between B:A=1:1 and B:A=1:3 co-cultures *in vivo* (data not shown). Angiogenesis was estimated by counting CD31-positive vessels in the tumor; however, no significant difference was observed (data not shown).

Discussion

The present study demonstrated that BxPC-3 cells co-cultured with rich ASF-4-1 cells acquired chemoresistance, invasive properties and increased mTOR expression *in vitro*. Furthermore, fibroblast-rich culture promoted tumor growth and invasion *in vivo*. This indicates that rich ASF-4-1 cells promote the malignant potential of BxPC-3 cells *in vitro* and *in vivo*.

In colon cancer and early breast cancer, the enrichment of stromal cells within the primary tumor has been observed to be correlated with poor prognosis (4,5). In addition, various studies have concluded that the microenvironment surrounding cancer cells promotes cancer progression (6,7). Fibroblasts, in particular, support tumor growth and promote metastasis and drug resistance (21,22). Therefore, we hypothesized that a fibroblast-enriched microenvironment would promote the malignant potential of the pancreatic cancer cell line BxPC-3.

Tumor budding is an independent prognostic factor in pancreatic cancer as well as other cancer types, particularly colorectal cancer (12-14). Budding cells are defined as small clusters that are de-differentiated and located around the invasive front (11,12). These cells are CK18-positive and suppress E-cadherin; therefore, they are thought to undergo EMT, resulting in malignant progression (16). In the current study, budding cells were observed around the invasive front in B:A=1:3 co-cultures. When BxPC-3 cells migrated into the Matrigel-collagen mixture, they appeared to have suppressed E-cadherin expression following their interaction with fibroblasts, a process that may lead to tumor budding. Under fibroblast-rich conditions, the number of BxPC-3 cells at the invasive front decreased compared with the B:A=1:1 co-cultures. Tumor budding is observed in pancreatic cancer in addition to gastrointestinal carcinoma (11). In the present study, co-culture with a high ratio of fibroblasts led BxPC-3 to initiate tumor budding and possibly EMT.

The atypical serine/threonine protein kinase mTOR belongs to the phosphoinositide-3 kinase (PI3K)-related kinase family. mTOR forms two distinct complexes, named mTOR complex (mTORC) 1 and 2 (18), by interacting with a number of proteins. The mTORC1 pathway integrates at least five major types of intracellular and extracellular signals (growth factors, stress, energy status, oxygen and amino acid signals) to control various major processes, including protein and lipid synthesis, autophagy, proliferation, metabolism and cell growth (18). In cancer cells, mTORC1 controls apoptosis and angiogenesis through hypoxia-inducible factor 1 and vascular endothelial growth factor, and cell mobility through the RhoA-Rac1 pathway (23,24). The mTORC2 pathway integrates growth factors and controls metabolism, cytoskeletal organization and cell survival (18). Thus, mTOR controls cell size in addition to certain major signals in cancer cells, affecting invasion, proliferation and migration. In the current study, the mean size of the cells at the invasive front in B:A=1:3 co-cultures was larger than that in B:A=1:1 co-cultures *in vitro*. In addition, BxPC-3 cells at the invasive front expressed a higher level of mTOR in B:A=1:3 co-cultures than did those in B:A=1:1 co-cultures *in vitro*. Furthermore, rapamycin, an mTOR inhibitor, prevented BxPC-3 cells in B:A=1:3 co-cultures from migrating and proliferating.

mTOR is involved in chemoresistance in pancreatic cancer through an apoptotic pathway including nuclear factor κB and the Akt/PI3K pathway (25,26). In the current study, an elevated fibroblast ratio increased chemoresistance of BxPC-3 cells to gemcitabine at the invasive front. BxPC-3 cells in the B:A=1:3 co-cultures may have suppressed apoptosis through the Akt/PI3K pathway, resulting in increased chemoresistance. mTOR is downstream from the Akt pathway. It has been shown that proliferation, invasion and colony formation by BxPC-3 cells are promoted through activation of mitogen-activated protein kinase (MAPK) and Akt pathways by human pancreatic stellate cells (8). In the present study, it is suggested that the Akt/PI3K pathway in BxPC-3 cells may have been activated in the presence of high ratios of ASF-4-1 cells, resulting in activation of mTOR. Consistently, in fibroblast-rich culture, mTOR expression correlated with malignant potential of BxPC-3 cells.

In penile squamous cell carcinoma, mTOR has been shown to be overexpressed in histologically high grade cases (27). BxPC-3 cells with enriched fibroblasts may have been in a histologically high grade due to mTOR expression at the time of transplantation. In addition, neural invasion of pancreatic cancer is correlated with phosphorylation of the RET-Ras-MAPK pathway (28). As mTOR is downstream from the Ras signal (18), in the current xenograft model, BxPC-3 cells from B:A=1:3 co-cultures may have had the ability for neural invasion when they were transplanted.

There was no significant change in mTOR expression in B:A=1:1 co-cultures or B:A=1:3 co-cultures used for xenografting. It is possible that, following transplantation, mTOR expression in BxPC-3 cells was induced by some other factor, e.g., growth factors, cytokines, hormones, blood flow or immunoregulation (18).

In the present study, the model tissue had no blood flow and no immune response, which limited these results with regard to the accuracy of mimicking of the pancreatic cancer microenvironment *in vivo*. However, we suggest that this model may be useful for cancer research, particularly studies of the interaction between cancer cells and fibroblast enrichment, and the mechanisms of tumor proliferation and invasion. Because the passages of the cell lines were different, the ratio between cancer cells and fibroblast cells may be altered due to their different growth rate. However, the same experiments were repeated at least three times with cells from different passages, yielding almost identical Ki-67 indices; therefore, the difference of passages exerts little influence on the result. In the future, we aim to investigate the interactions with endothelial cells, immune cells, other cell lines and pancreatic cancer cells derived from the human body.

References

1. Jemal A, Bray F, Center MM, Ferlay J, Ward E and Forman D: Global cancer statistics. CA Cancer J Clin 61: 69-90, 2011.
2. Wolfgang CL, Herman JM, Laheru DA, Klein AP, Erdek MA, Fishman EK and Hruban RH: Recent progress in pancreatic cancer. CA Cancer J Clin 63: 318-348, 2013.
3. Hidalgo M: Pancreatic cancer. N Engl J Med 362: 1605-1617, 2010.
4. de Kruijf EM, van Nes JG, van de Velde CJ, Putter H, Smit VT, Liefers GJ, Kuppen PJ, Tollenaar RA and Mesker WE: Tumor-stroma ratio in the primary tumor is a prognostic factor in early breast cancer patients, especially in triple-negative carcinoma patients. Breast Cancer Res Treat 125: 687-696, 2011.
5. Mesker WE, Junggeburt JM, Szuhai K, de Heer P, Morreau H, Tanke HJ and Tollenaar RA: The carcinoma-stromal ratio of colon carcinoma is an independent factor for survival compared to lymph node status and tumor stage. Cell Oncol 29: 387-398, 2007.
6. Dunér S, Lopatko Lindman J, Ansari D, Gundewar C and Andersson R: Pancreatic cancer: The role of pancreatic stellate cells in tumor progression. Pancreatology 10: 673-681, 2010.
7. Liotta LA and Kohn EC: The microenvironment of the tumour-host interface. Nature 411: 375-379, 2001.
8. Hwang RF, Moore T, Arumugam T, Ramachandran V, Amos KD, Rivera A, Ji B, Evans DB and Logsdon CD: Cancer-associated stromal fibroblasts promote pancreatic tumor progression. Cancer Res 68: 918-926, 2008.
9. Gaggioli C, Hooper S, Hidalgo-Carcedo C, Grosse R, Marshall JF, Harrington K and Sahai E: Fibroblast-led collective invasion of carcinoma cells with differing roles for RhoGTPases in leading and following cells. Nat Cell Biol 9: 1392-1400, 2007.
10. Lin RZ and Chang HY: Recent advances in three-dimensional multicellular spheroid culture for biomedical research. Biotechnol J 3: 1172-1184, 2008.
11. Karamitopoulou E, Zlobec I, Born D, Kondi-Pafiti A, Lykoudis P, Mellou A, Gennatas K, Gloor B and Lugli A: Tumour budding is a strong and independent prognostic factor in pancreatic cancer. Eur J Cancer 49: 1032-1039, 2013.
12. Ueno H, Price AB, Wilkinson KH, Jass JR, Mochizuki H and Talbot IC: A new prognostic staging system for rectal cancer. Ann Surg 240: 832-839, 2004.
13. Prall F: Tumour budding in colorectal carcinoma. Histopathology 50: 151-162, 2007.
14. Koike M, Kodera Y, Itoh Y, Nakayama G, Fujiwara M, Hamajima N and Nakao A: Multivariate analysis of the pathologic features of esophageal squamous cell cancer: Tumor budding is a significant independent prognostic factor. Ann Surg Oncol 15: 1977-1982, 2008.
15. Landau MS, Hastings SM, Foxwell TJ, Luketich JD, Nason KS and Davison JM: Tumor budding is associated with an increased risk of lymph node metastasis and poor prognosis in superficial esophageal adenocarcinoma. Mod Pathol 27: 1578-1589, 2014.
16. Zlobec I and Lugli A: Epithelial mesenchymal transition and tumor budding in aggressive colorectal cancer: Tumor budding as oncotarget. Oncotarget 1: 651-661, 2010.
17. Karamitopoulou E: Role of epithelial-mesenchymal transition in pancreatic ductal adenocarcinoma: Is tumor budding the missing link? Front Oncol 3: 221, 2013.
18. Laplante M and Sabatini DM: mTOR signaling in growth control and disease. Cell 149: 274-293, 2012.
19. Arlt A, Müerköster SS and Schäfer H: Targeting apoptosis pathways in pancreatic cancer. Cancer Lett 332: 346-358, 2013.
20. Leers MP, Kölgen W, Björklund V, Bergman T, Tribbick G, Persson B, Björklund P, Ramaekers FC, Björklund B, Nap M *et al*: Immunocytochemical detection and mapping of a cytokeratin 18 neo-epitope exposed during early apoptosis. J Pathol 187: 567-572, 1999.
21. Tod J, Jenei V, Thomas G and Fine D: Tumor-stromal interactions in pancreatic cancer. Pancreatology 13: 1-7, 2013.
22. Feig C, Gopinathan A, Neesse A, Chan DS, Cook N and Tuveson DA: The pancreas cancer microenvironment. Clin Cancer Res 18: 4266-4276, 2012.
23. Shen K, Ji L, Gong C, Ma Y, Yang L, Fan Y, Hou M and Wang Z: Notoginsenoside Ft1 promotes angiogenesis via HIF-1α mediated VEGF secretion and the regulation of PI3K/AKT and Raf/MEK/ERK signaling pathways. Biochem Pharmacol 84: 784-792, 2012.
24. Tan CY and Hagen T: Post-translational regulation of mTOR complex 1 in hypoxia and reoxygenation. Cell Signal 25: 1235-1244, 2013.
25. Arlt A, Gehrz A, Müerköster S, Vorndamm J, Kruse ML, Fölsch UR and Schäfer H: Role of NF-kappaB and Akt/PI3K in the resistance of pancreatic carcinoma cell lines against gemcitabine-induced cell death. Oncogene 22: 3243-3251, 2003.
26. Hamacher R, Schmid RM, Saur D and Schneider G: Apoptotic pathways in pancreatic ductal adenocarcinoma. Mol Cancer 7: 64, 2008.
27. Chaux A, Munari E, Cubilla AL, Hicks J, Lecksell K, Burnett AL and Netto GJ: Immunohistochemical expression of the mammalian target of rapamycin pathway in penile squamous cell carcinomas: A tissue microarray study of 112 cases. Histopathology 64: 863-871, 2014.
28. Gil Z, Cavel O, Kelly K, Brader P, Rein A, Gao SP, Carlson DL, Shah JP, Fong Y and Wong RJ: Paracrine regulation of pancreatic cancer cell invasion by peripheral nerves. J Natl Cancer Inst 102: 107-118, 2010.